

Supplementary Figures

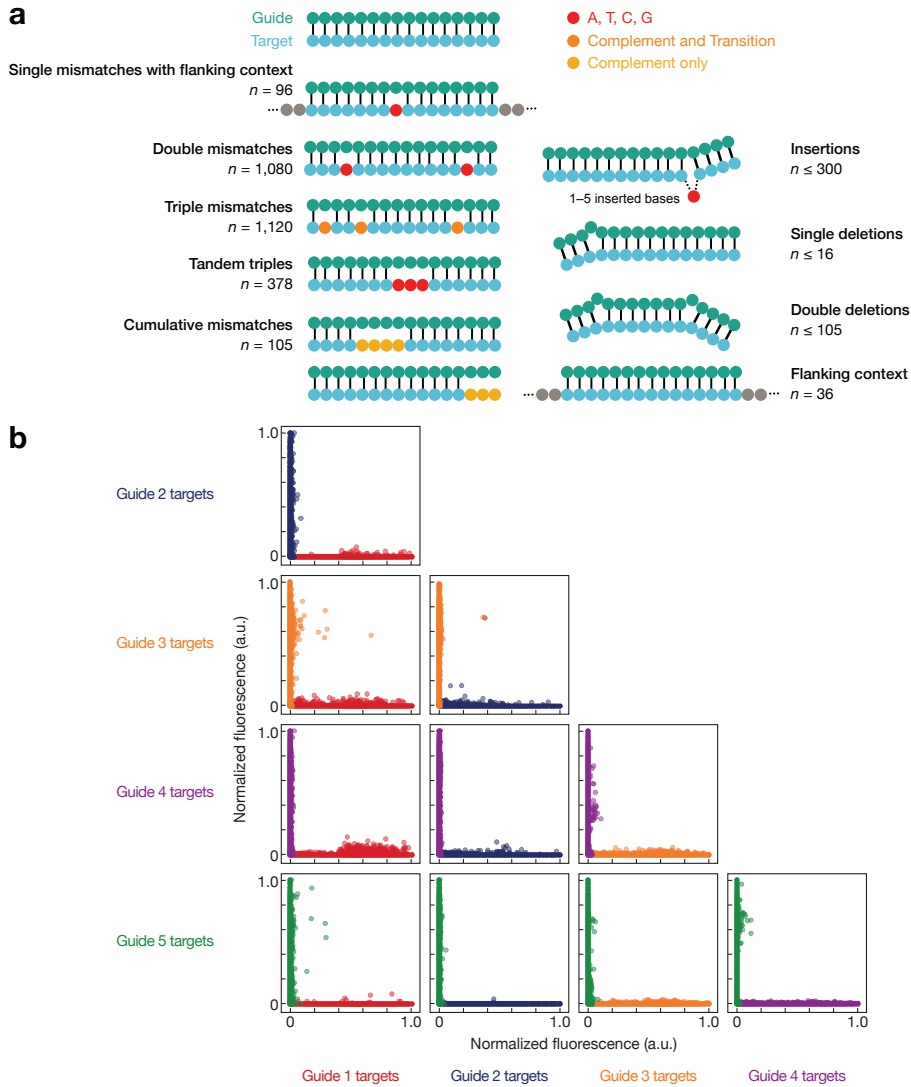
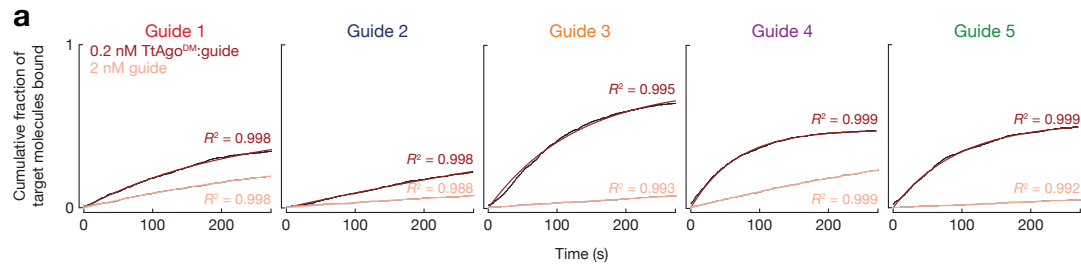


Figure S1 | Library design and construction, Related to Figure 1 **(a)** Schematic of designed targets included in libraries of each of the five TtAgo guides. **(b)** Demonstration of specificity of individually flowed TtAgo^{DM}:guide complexes for corresponding target libraries (800 pM each TtAgo^{DM}:guide at equilibrium). *x* and *y* axes show the normalized fit maximum fluorescence of the indicated target library.



k_{on} ($M^{-1} s^{-1}$)

$2.3 \pm 0.01 \times 10^7$	$0.59 \pm 0.01 \times 10^7$	$8.9 \pm 0.01 \times 10^7$	$7.5 \pm 0.01 \times 10^7$	$5.3 \pm 0.01 \times 10^7$
$1.4 \pm 0.01 \times 10^6$	$0.94 \pm 0.01 \times 10^6$	$0.49 \pm 0.01 \times 10^6$	$0.92 \pm 0.01 \times 10^6$	$0.37 \pm 0.01 \times 10^6$

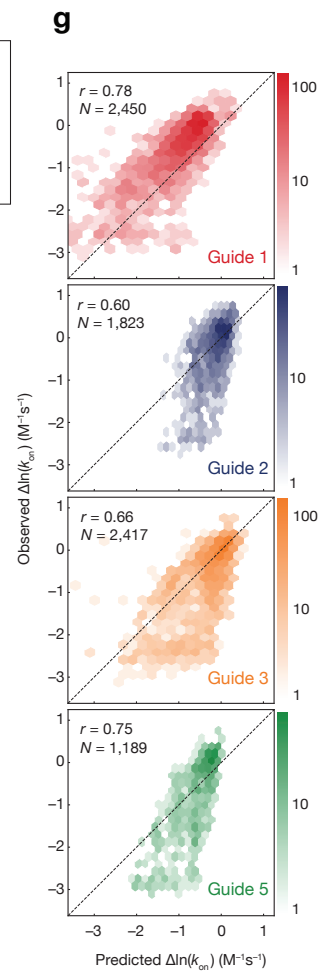
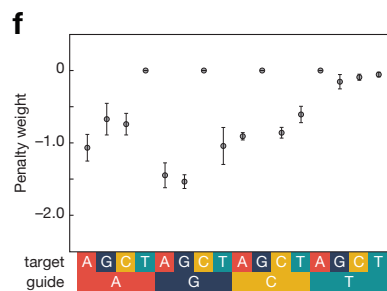
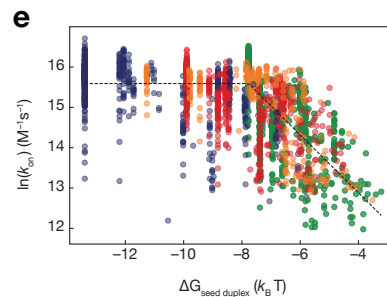
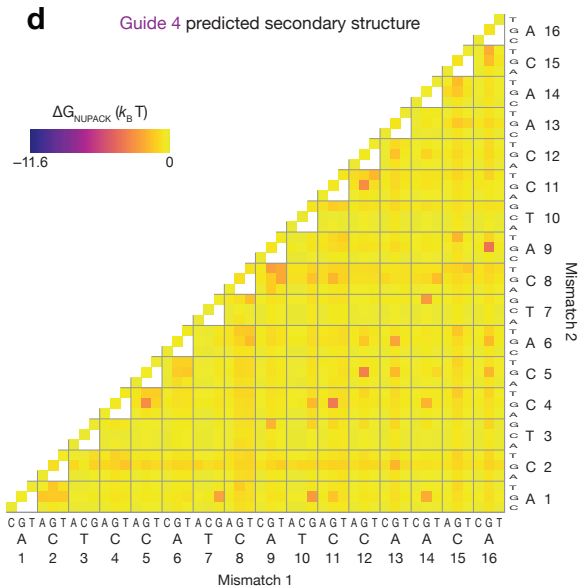
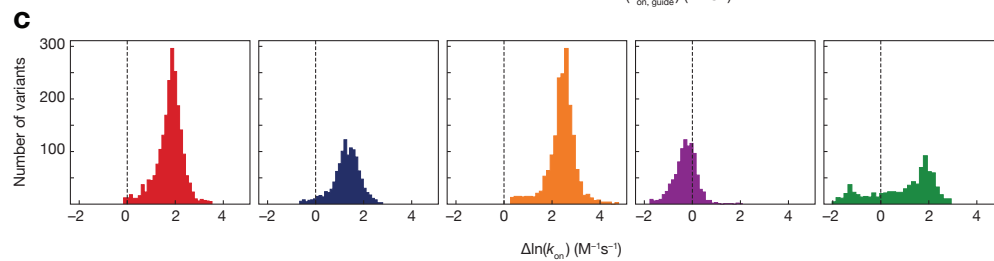
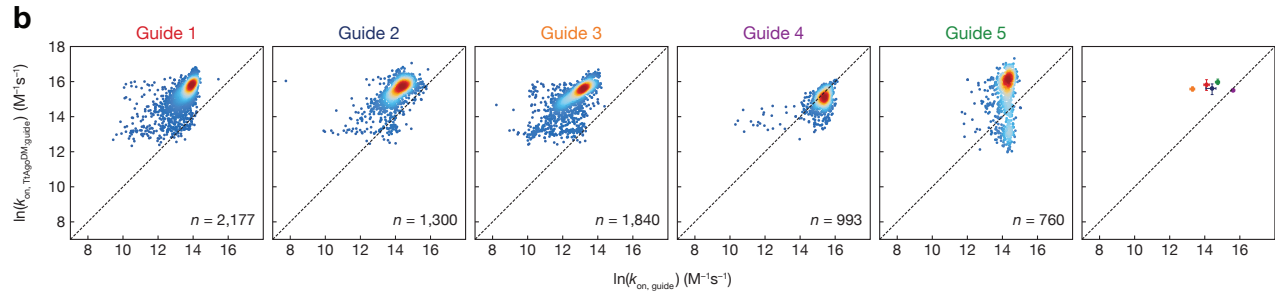


Figure S2 | Factors contributing to the association kinetics, Related to Figure 2 (a) Cumulative fraction of TtAgo^{DM}:guide or unloaded guide molecules binding for the first time to a fully complementary, single DNA target measured by Co-localization single-molecule spectroscopy. Data points are plotted in black (TtAgo^{DM}:guide) and gray (guide alone), and the curves show the rate of binding after correcting for non-specific association of TtAgo^{DM}:guide (red) or guide alone (salmon) with the glass surface. The binding rate (k_{on}) was determined by fitting the cumulative fractions of arrivals to $f(t) = 1 - (1 - h) \times e^{-k_{on} \times t} - h \times e^{-(k_{on} + k_{NS}) \times t}$ and reported per time unit and concentration of introduced TtAgo^{DM}:guide (0.2 nM) or guide alone (2 nM). Parameters relative to non-specific association with the glass surface (k_{NS} , on-rate for non-specific arrivals; h , fraction of control locations having received non-specific arrivals) were determined from the fitting of data for control locations. Values of k_{on} were derived from data collected from >1,000 individual DNA target molecules; standard error from bootstrapping is reported. (b) Association rate constants of unloaded DNA guides (x-axis) and TtAgo^{DM} (y-axis) for all library targets. The right plot shows association rate constants for fully complementary targets of each guide, and error bars indicate the 95% confidence interval on the fit association rate constant. (c) The difference in association rate constants between guide-loaded TtAgo^{DM} and unloaded guides for targets shown in (b). (d) The NUPACK predicted secondary structure for targets of guide 4 containing single and double mismatches. (e) The relationship between the NUPACK predicted seed energy (5-mer beginning at t2) and the measured TtAgo^{DM} association rate constant. Points are colored by guide. The dotted trendline was generated using piecewise linear regression with the first segment constrained to have a slope of 0. (f) Guide to target mismatch penalty weights, related to Fig. 2d. Error bars indicate SEM of penalty weights across models fit with each guide held out in turn ($n = 4$). (g) Comparison of

model predicted TtAgo^{DM} relative association rates to observed relative association rates for guides not used in model training, i.e. leave-one-out cross validation. Color bar indicates the number of targets in each bin.

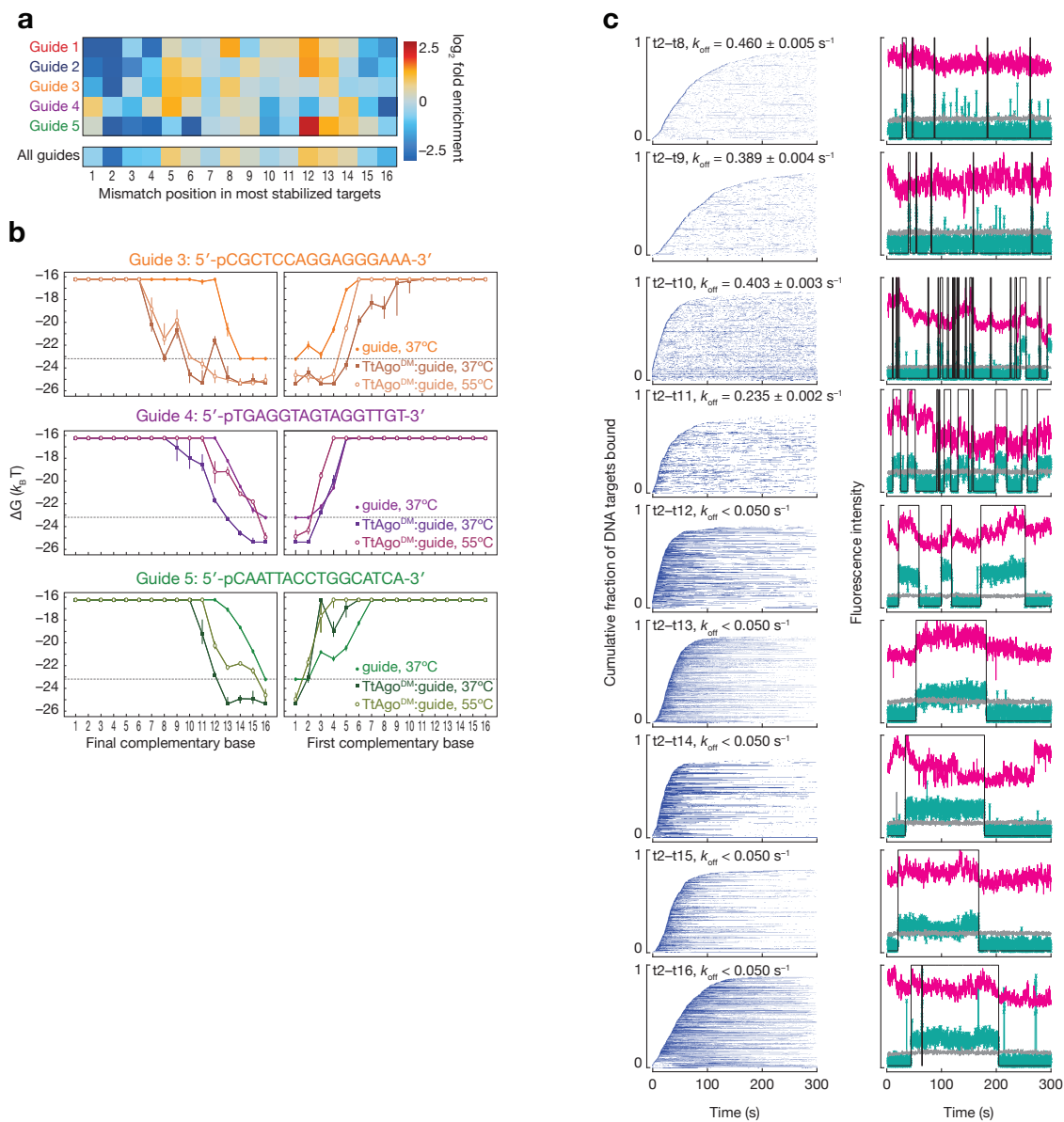


Figure S3 | Factors contributing to binding affinities, Related to Figure 3 (a) Enrichment of mismatch positions in the 10% of most TtAgo-stabilized targets, relative to all measured targets. (b) Binding energies for targets of guides 3, 4, and 5 containing progressively more complementarity to the DNA guide. Target mismatches progress from the 5' end (left panel) or the 3' end (right panel) of the target. Error bars indicate the 95% confidence interval on the

binding energy. The dotted line indicates the minimum measurable binding affinity for unloaded guide. (c) Single-molecule analysis of TtAgo^{DM}:guide 4 (turquoise) binding DNA targets (magenta) with different extents of complementarity to the guide DNA at 37°C. Left: rastergram summary of traces of individual target molecules, each in a single row and sorted according to their arrival time, for different guide:target pairings. Right: representative fluorescence intensity time traces. Light gray indicates background levels of green fluorescence, whereas the black line denotes binding events. Values of k_{off} were derived from data collected from >300 individual DNA target molecules; standard error from bootstrapping is reported. Values of k_{off} were not determined for t2–t12, t2–t13, t2–t14, t2–15, and t2–t16 targets because their k_{off} was slower than the rate of photobleaching (0.050 s^{-1}).

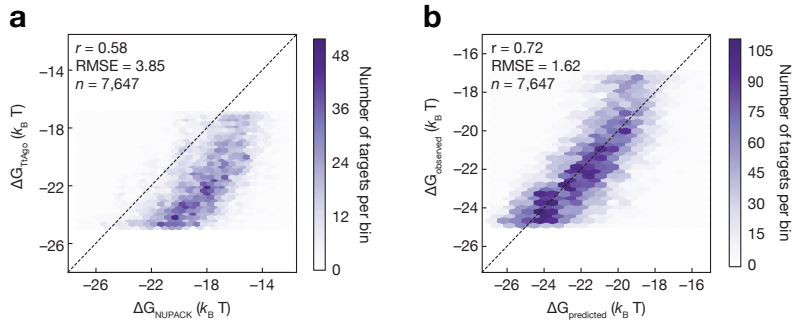


Figure S4 | Predictive model for TtAgo binding, Related to Figure 4 **(a)** Comparison of binding energies predicted by NUPACK to the observed binding energies. **(b)** Comparison of binding affinities predicted by the transition-transversion model to the observed binding affinity when trained on all data.

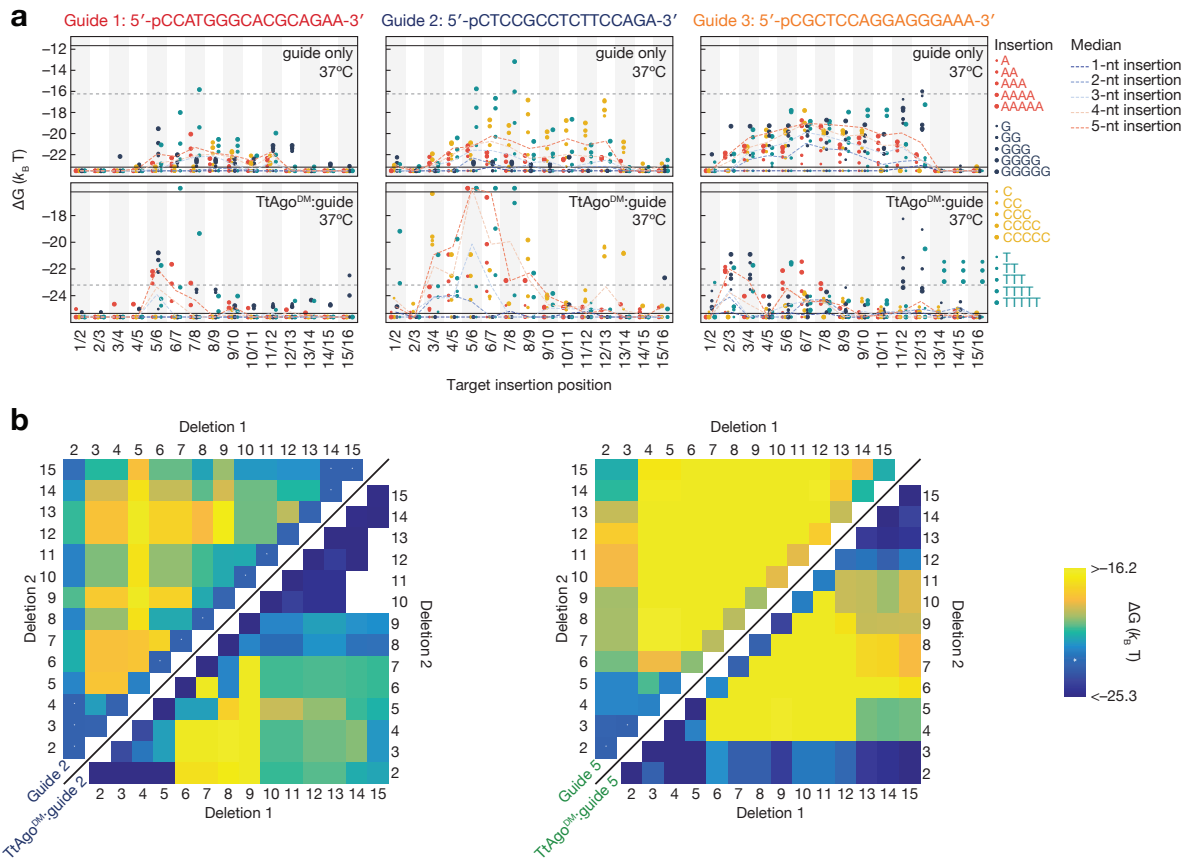


Figure S5 | Effect of insertions and deletions of target nucleotides on binding energy, Related to Figure 5 (a) Binding energies for unloaded guide (top) and TtAgo^{DM}:guide (bottom) at 37°C to targets with 1- to 5-nt insertions. Axes are labeled with the 3' end of the target (5' end of the guide) starting at position 1. Horizontal black lines indicate the limits of detection, and points below the bottom black line bound with higher affinity than the detection limit. The horizontal grey dotted lines in the unloaded guide plots indicate the TtAgo^{DM} upper limit of detection and the horizontal grey lines in the TtAgo^{DM} plots indicate the lower limit of detection for the unloaded guide. (b) Binding energies of unloaded guide (upper left) and TtAgo^{DM}:guide (lower

right) to DNA targets with single and double deletions at 37°C. White asterisks on the upper left heatmap indicate the minimum measurable binding affinity for the unloaded guide.

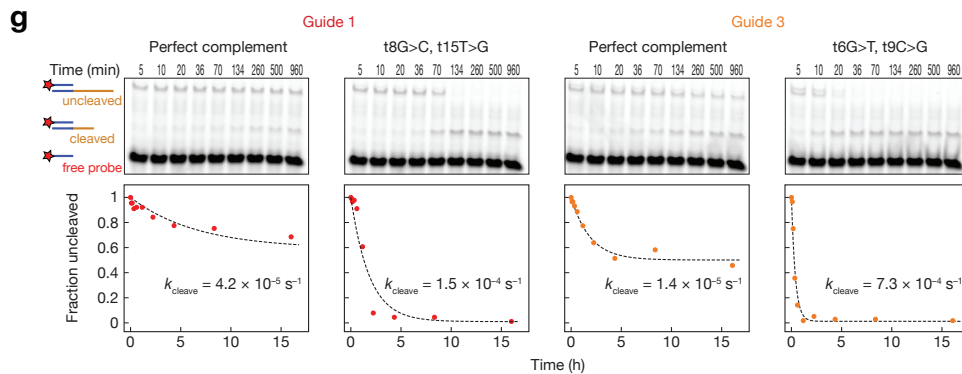
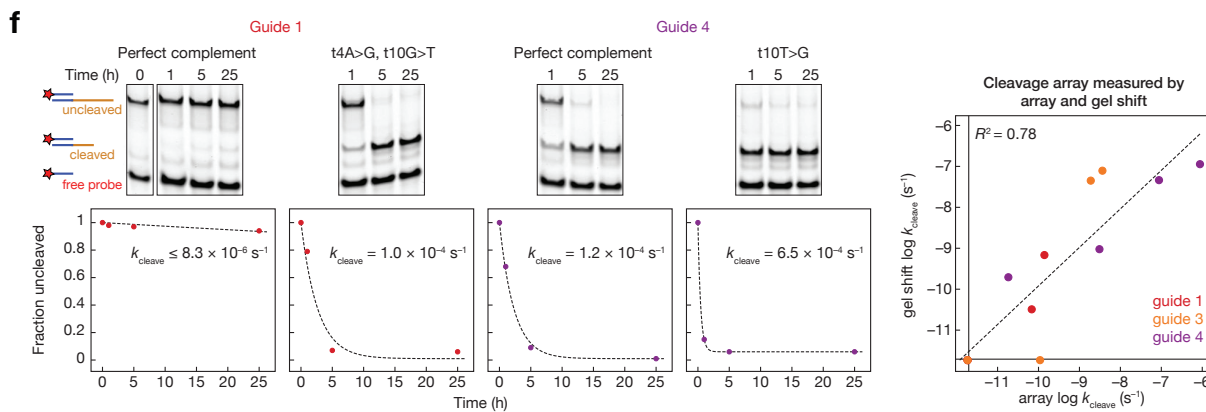
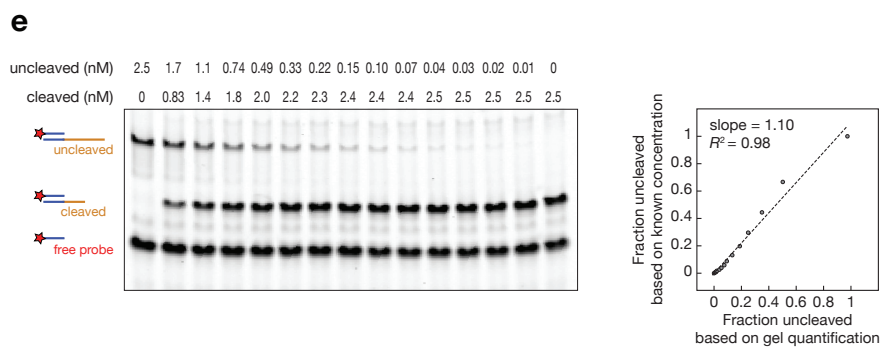
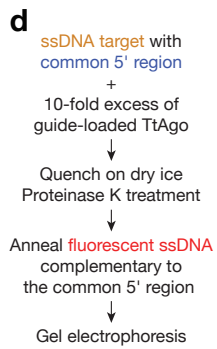
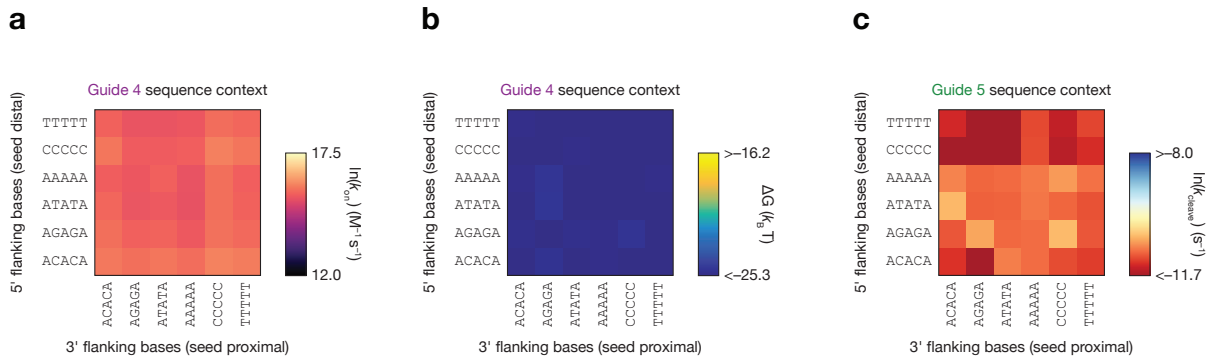


Figure S6 | Factors contributing to cleavage rates, Related to Figure 6 (a) The effect of flanking sequence context on the association rate constant of fully complementary guide 4 targets. (b) The effect of flanking sequence context on the binding affinity of fully complementary guide 4 targets. (c) The effect of flanking sequence context on the cleavage rate of fully complementary guide 5 targets. (d) Gel shift experimental method to validate single turnover cleavage rates for single targets. After cleaving for variable lengths of time, full length targets and cleaved product are visualized with a fluorescently labeled probe complementary to a common region ssDNA targets. (e) Demonstration of signal linearity of gel shift experiment in (d) using a dilution series of full length and cleaved targets. (f) Selected examples of mismatched targets that cleave faster than the corresponding fully complementary target. Cleavage performed in Mg^{2+} -containing buffer at 55°C. Right panel shows correlation between gel shift cleavage rate fit values and array fit values. (g) Selected examples of mismatched targets that cleave faster than the corresponding fully complementary target. Cleavage performed in Mn^{2+} -containing buffer at 65°C.

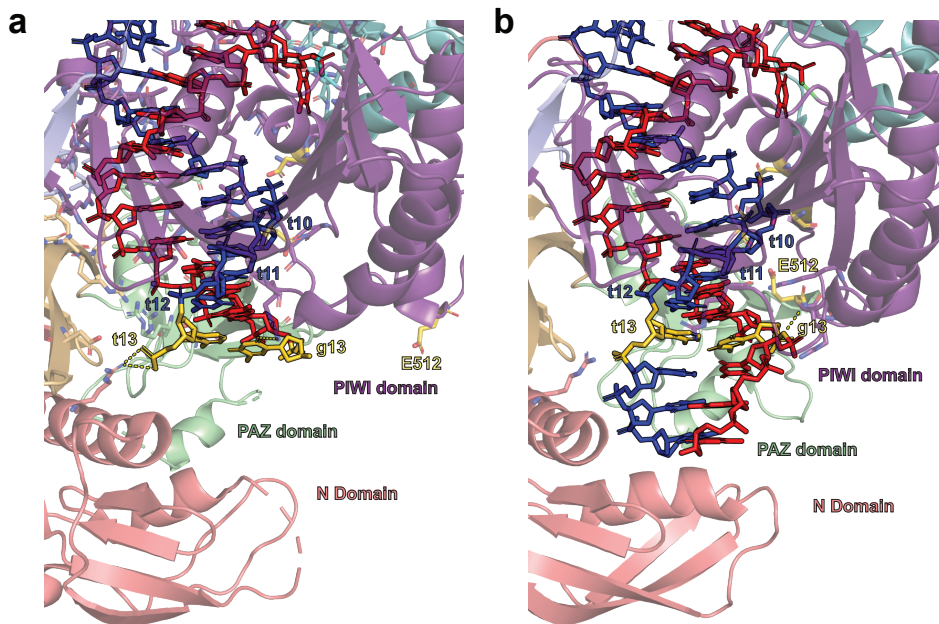


Figure S7 | Structural determinants of TtAgo cleavage activity, Related to Figure 6 (a) TtAgo crystal structure with a 15-mer DNA target in the cleavage incompatible conformation (PDB 4N41). Target position 13 (t13) and guide position 13 (t13) are both colored yellow, while the rest of the target strand is colored blue and the guide strand red. Catalytic residue E512 is labeled yellow, as are catalytic residues D478, D546, and D660. Dashed lines indicate predicted hydrogen bonds between either the guide or target strand and TtAgo. (b) TtAgo crystal structure with a 16-mer DNA target in the cleavage compatible conformation (PDB 4NCA). Coloring and labels as in (a).